Supporting Information

Pseudo Spin Valve Behavior in Colloidally Prepared Nanoparticle Films

Benjamin H. Zhou[1] and Jeffrey D. Rinehart*[1,2]

[1]Materials Science and Engineering Program and [2]Department of Chemistry and Biochemistry, University of California – San Diego, La Jolla, CA 92093, USA.

*jrinehart@ucsd.edu

Materials

The nanoparticle synthesis reagents used were cobalt(II) chloride hexahydrate (98%, Sigma Aldrich), iron(III) chloride hexahydrate (97% Alfa Aesar), sodium oleate (97% TCI), oleic acid (90%, Alfa Aesar), and 1-octadecene (90% Sigma Aldrich). Nitrosonium tetrafluoroborate ($NOBF_4$, 98%) was purchased from Alfa Aesar. HPLC grade dichloromethane (DCM), and ACS grade acetone, hexane, ethanol, isopropanol and toluene were purchased from Fisher. ACS grade Dimethyl formamide (DMF) was purchased from EMD Millipore. All chemicals were used as received.

Synthesis of metal oleate precursors

The iron oleate and cobalt/iron mixed oleate were synthesized according to literature procedures.[1-2] Iron(III) chloride hexahydrate (8.1 g, 30 mmol) and sodium oleate (27.4 g, 90 mmol), or a 1:2 molar mixture of cobalt(II) chloride hexahydrate (2.4 g, 10 mmol) and iron(III) chloride hexahydrate (5.4 g, 20 mmol) and sodium oleate (24.4 g, 80 mmol) were combined in a solvent mixture of water (45 mL), ethanol (60 mL), and hexane (105 mL). This reaction mixture was brought to reflux (60°C) for 4 h. After being cooled to room temperature, the upper organic layer was washed with water (30 mL) three times. Finally, hexane was evaporated from the product, leaving the viscous, oily metal oleate complex. The cobalt/iron mixed oleate was aged for a month in the dark at room temperature before being used in nanoparticle synthesis.

Synthesis of $CoFe_2O_4$ and Fe_3O_4 nanoparticles

$CoFe_2O_4$ and Fe_3O_4 nanoparticles were synthesized according to modified literature procedures.[1-3] Iron or cobalt/iron oleate (1.4 mmol) was mixed with oleic acid (0.2 g, 0.7 mmol for $CoFe_2O_4$, 1 g, 3.5 mmol for Fe_3O_4) and 1-octadecene (7 g) in a 50 mL three-neck Morton flask. The reaction mixture was degassed under vacuum at 110°C for 1 h, after which the atmosphere was back-filled with dinitrogen. Throughout the rest of the reaction, 100 sccm of dinitrogen was flowed through the reaction system into a side neck of the Morton flask and out the condenser attached to the middle neck. The reaction mixture was heated to 320°C at 3°C/min, where it was refluxed for 0.5 h then cooled to room temperature. When the temperature reached 318°C, 5 sccm of dioxygen was added to the dinitrogen stream and flowed continuously to the end of the reaction.

The resulting nanoparticles were isolated from the other reaction byproducts by addition of hexane (25 mL) and ethanol (40 mL). The nanoparticles were collected by centrifugation at 8500 rpm and redispersed in hexane (10 mL). After another cycle of precipitation with ethanol and centrifugation, the nanoparticles were stored in hexane.

Ligand exchange of nanoparticles and deposition into films

The nanoparticles were stripped of their long-chain organic ligands according to a modified literature procedure.[4] Hexane suspensions of $CoFe_2O_4$ and Fe_3O_4 nanoparticles were diluted to 4 mg/mL. The two suspensions were then mixed in 1:3, 1:1, and 3:1 ratios by volume. A 1 mL aliquot of each hexane suspension was concentrated by evaporating approximately half the volume of hexane with flowing dinitrogen. About 2 mL of a saturated solution of $NOBF_4$ in DCM was added to the concentrated suspension, which was then shaken until the nanoparticles visibly flocculated. The nanoparticles were collected with a magnet and the supernatant was discarded; they were then redispersed in DMF and precipitated out by addition of toluene. This final precipitate was redispersed in DMF (1 mL) at a concentration of 4 mg/mL for storage and deposition.

Substrates with gold electrode patterns were cleaned by a 10 min. sonication each in acetone then isopropanol. The substrates were dried and placed on a 60°C hotplate. 3 μL of a DMF suspension of a given nanoparticle mixture was then dropcast onto a substrate, drying within a few minutes. The films were then fully dried under vacuum at 150°C for 1.5 h

Deposition of gold electrodes on silicon substrates

Gold electrodes on silicon substrates were patterned at the Nano3 cleanroom at the San Diego Nanotechnology Infrastructure (SDNI) of UCSD. AZ1518MIF photoresist was spun onto a 4" silicon wafers with 300 nm of thermal oxide. The wafer was exposed to the pattern in Figure S2, on a Karl Suss MA6 Mask Aligner and developed with AZ MIF 300. Finally, approximately 10 nm of a Ti adhesion layer and 100 nm of Au were sputtered onto the wafer in an AJA DC sputter deposition tool, with final lift-off done in acetone.

Characterization

Transmission electron microscopy (TEM) was performed with an FEI Spirit TEM operating at 120kV, with images collected by a 2k x 2k Gatan CCD camera. Samples were prepared by air-drying a dilute hexane solution of nanoparticles on carbon-coated copper grids. Particle sizes were analyzed using ImageJ using the Huang thresholding algorithm on sample sizes of N = 747, and 3,578 for $CoFe_2O_4$ and Fe_3O_4.[5] Scanning electron microscopy (SEM) and energy-dispersive X-ray spectroscopy (EDS) was performed with a Zeiss Sigma 500. Magnetic and magnetoelectric measurements were performed using a Quantum Design MPMS3 SQUID Magnetometer equipped with an Electrical Transport Option. Powder X-ray diffraction (XRD) was performed on a Bruker Diffractometer with a Mo K α radiation source and an Apex II Area Detector. The XRD patterns were fit using FullProf[6].

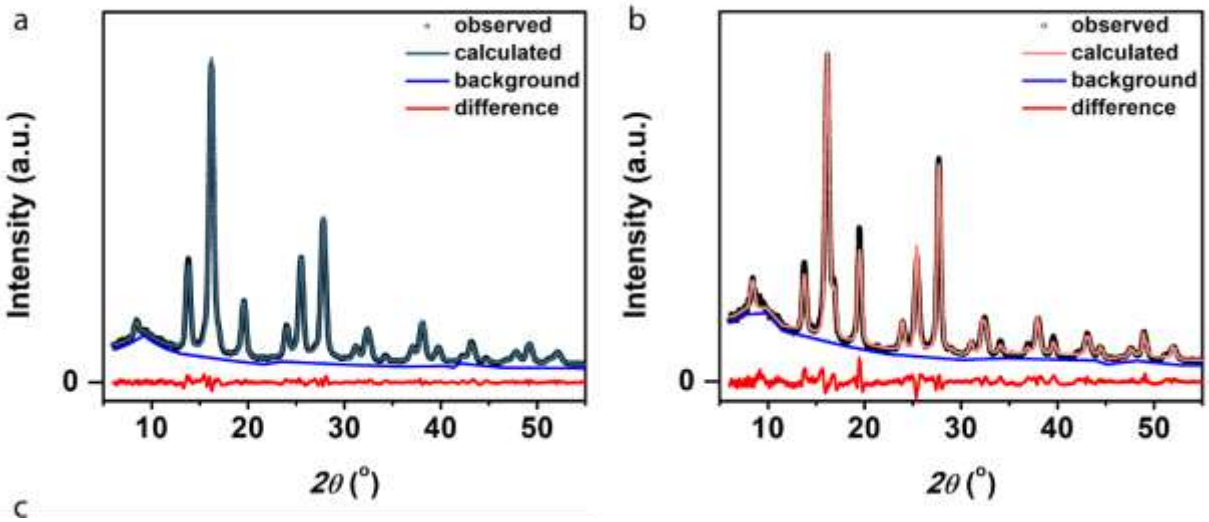

c

sample	R_b	R_{wp}	$a_{observed}$ (Å)	$a_{reference}$ (Å)	Difference in *a*
Fe_3O_4	1.76	5.74	8.357(3)	8.3941(7) (ICSD coll. code 26410)	−0.4384%
$CoFe_2O_4$	1.32	4.97	8.391(6)	8.3860(3) (ICSD coll. code 192790)	0.06642%

Figure S1. Powder X-ray diffraction patterns of a) Fe_3O_4 and b) $CoFe_2O_4$ nanoparticles. The patterns were fit by the Le Bail method in FullProf,[6-7] with the fit parameters shown in c).

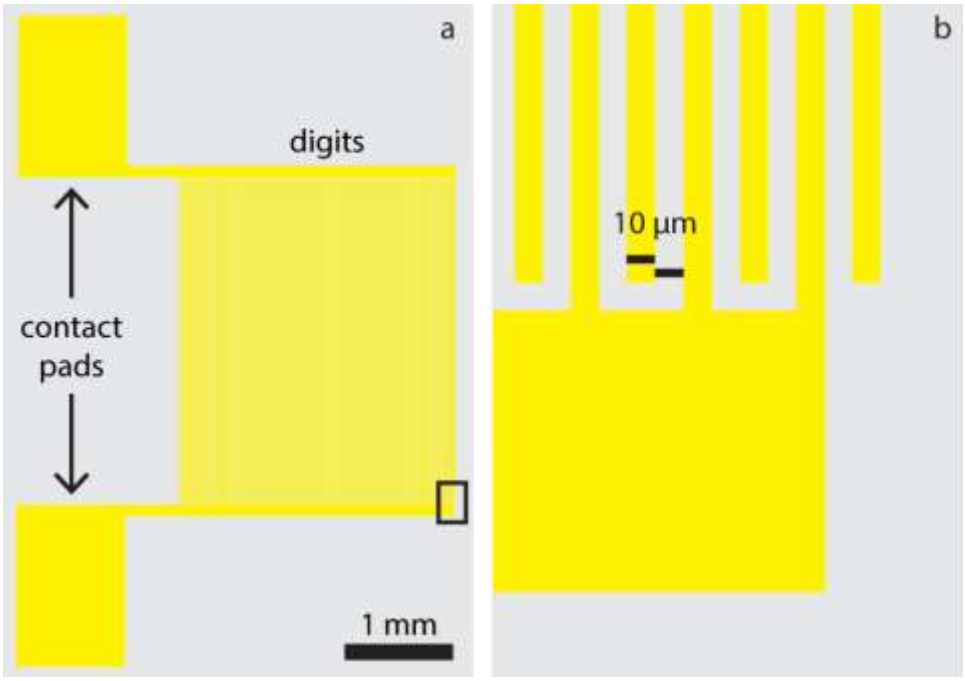

Figure S2. a) Overall schematic and b) detailed view (corresponding to the box in Figure S2a) of the interdigitated electrode pattern. The design consists of 64 digits per side, with 3 mm of overlapping length between digits. The spacing between the digits is 10 µm.

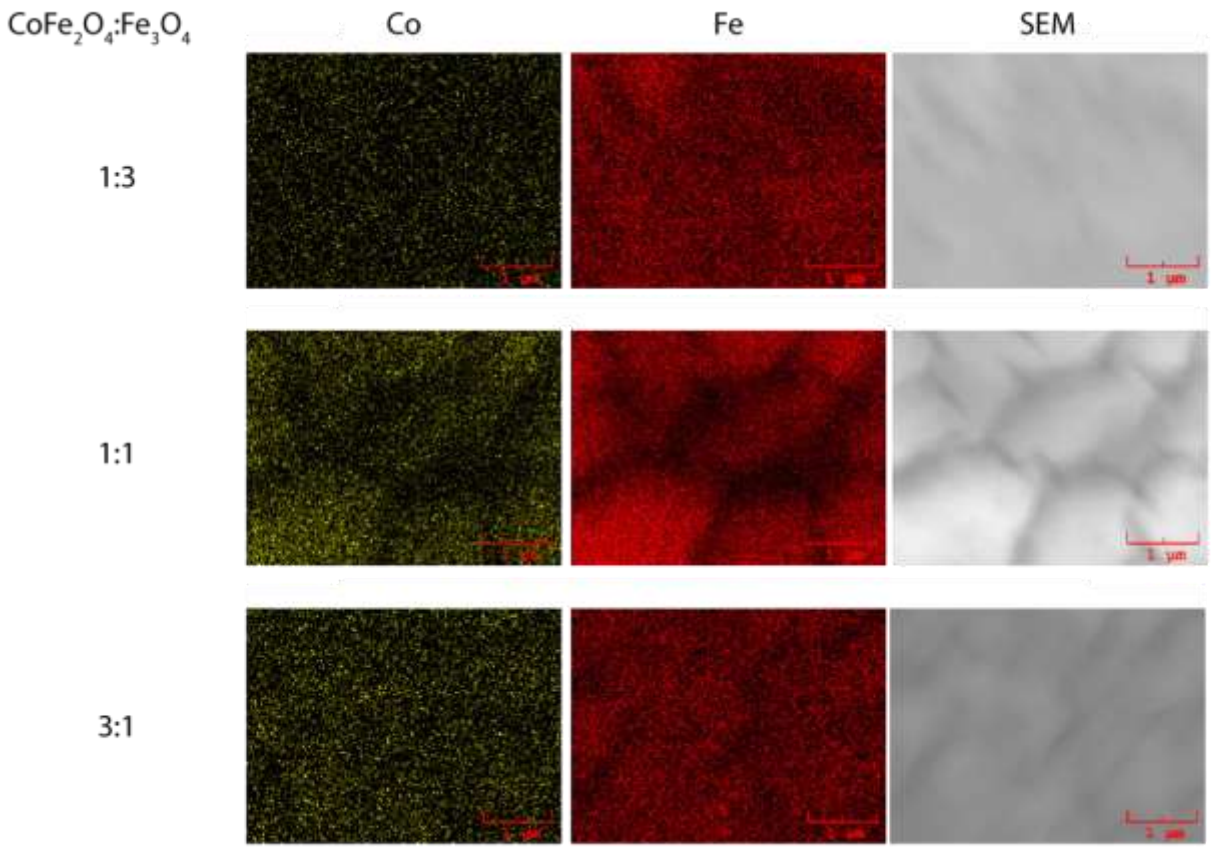

Figure S3. Energy dispersive X-ray spectroscopy element maps and corresponding scanning electron micrographs for the multi-component films.

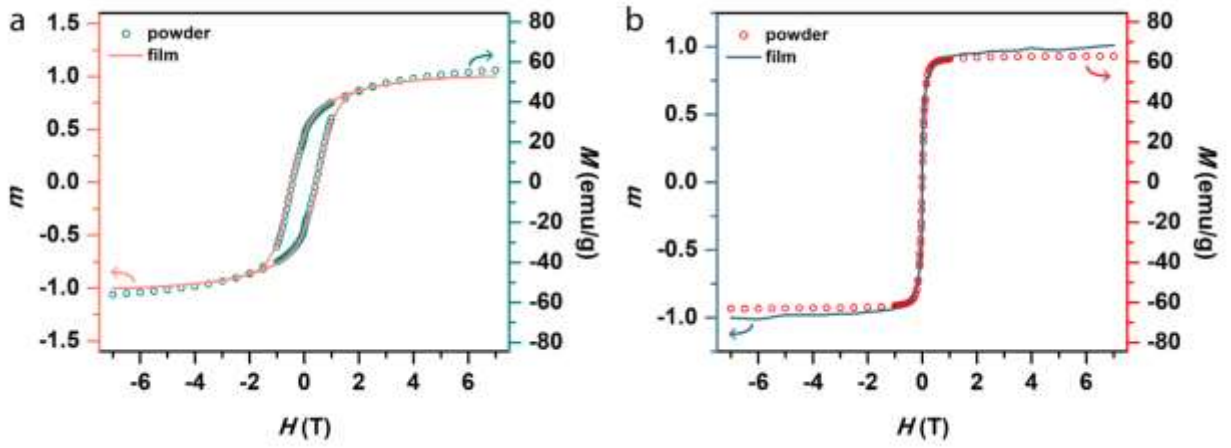

Figure S4. Magnetization and reduced magnetization vs magnetic field for a) $CoFe_2O_4$ and b) Fe_3O_4 nanoparticles. Circles and the right axes correspond to measurements performed on powders of the as-synthesized nanoparticles, while lines and the left axes correspond to measurements performed on the nanoparticles after ligand exchange and processing into films. The agreement between the powder and film data demonstrate the stability of the nanoparticles' properties throughout processing, as well as their retention of single particle properties. The powder and film data deviate from each other increasingly at larger fields; this is likely due to difficulty in accurately subtracting the diamagnetic contribution of the film substrate from the overall magnetic moment.

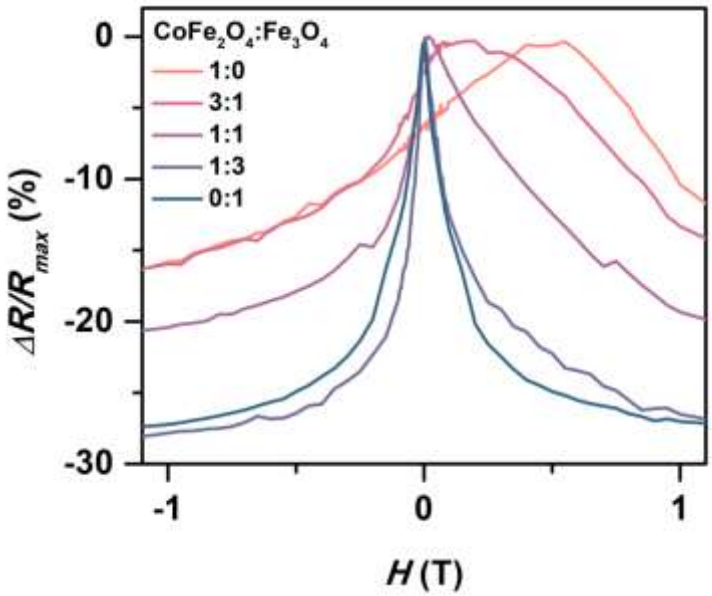

Figure S5. Overlaid plots of $\Delta R/R$ vs magnetic field (scanned from −7 to +7 T) at 200 K for each nanoparticle film. The combined figure emphasizes how sensitivity of the pure magnetite is improved through introduction of low-sensitivity cobalt ferrite due to the spin valve effect.

References

1. Park, J.; An, K. J.; Hwang, Y. S.; Park, J. G.; Noh, H. J.; Kim, J. Y.; Park, J. H.; Hwang, N. M.; Hyeon, T., Ultra-large-scale syntheses of monodisperse nanocrystals. *Nat. Mater.* 2004, *3* (12), 891-895.
2. Herrera, A. P.; Polo-Corrales, L.; Chavez, E.; Cabarcas-Bolivar, J.; Uwakweh, O. N. C.; Rinaldi, C., Influence of aging time of oleate precursor on the magnetic relaxation of cobalt ferrite nanoparticles synthesized by the thermal decomposition method. *J. Magn. Magn. Mater.* 2013, *328*, 41-52.
3. Unni, M.; Uhl, A. M.; Savliwala, S.; Savitzky, B. H.; Dhavalikar, R.; Garraud, N.; Arnold, D. P.; Kourkoutis, L. F.; Andrew, J. S.; Rinaldi, C., Thermal Decomposition Synthesis of Iron Oxide Nanoparticles with Diminished Magnetic Dead Layer by Controlled Addition of Oxygen. *ACS Nano* 2017, *11* (2), 2284-2303.
4. Dong, A.; Ye, X.; Chen, J.; Kang, Y.; Gordon, T.; Kikkawa, J. M.; Murray, C. B., A generalized ligand-exchange strategy enabling sequential surface functionalization of colloidal nanocrystals. *J. Am. Chem. Soc.* 2011, *133* (4), 998-1006.
5. Schneider, C. A.; Rasband, W. S.; Eliceiri, K. W., NIH Image to ImageJ: 25 years of image analysis. *Nat. Meth.* 2012, *9* (7), 671-675.
6. Rodríguez-Carvajal, J., Recent advances in magnetic structure determination by neutron powder diffraction. *Physica B: Condensed Matter* 1993, *192* (1-2), 55-69.
7. Le Bail, A., Whole powder pattern decomposition methods and applications: A retrospection. *Powder Diffr.* 2012, *20* (4), 316-326.